A Journal of the Gesellschaft Deutscher Chemiker
Angewandte Chemie
GDCh
International Edition
www.angewandte.org

Check for updates

Accepted Article

Title: Enabling Visible-Light-Driven Selective CO2 Reduction by Doping Quantum Dots: Trapping Electrons and Suppressing H2 Evolution

Authors: Jin Wang, Tong Xia, Lei Wang, Xusheng Zheng, Zeming Qi, Chao Gao, Junfa Zhu, Zhengquan Li, Hangxun Xu, and Yujie Xiong

To be cited as: *Angew. Chem. Int. Ed.* 10.1002/anie.201810550
Angew. Chem. 10.1002/ange.201810550

Link to VoR: http://dx.doi.org/10.1002/anie.201810550
http://dx.doi.org/10.1002/ange.201810550

WILEY-VCH

Enabling Visible-Light-Driven Selective CO_2 Reduction by Doping Quantum Dots: Trapping Electrons and Suppressing H_2 Evolution

Jin Wang,[a,b] Tong Xia,[a] Lei Wang,[a] Xusheng Zheng,[a] Zeming Qi,[a] Chao Gao,[a] Junfa Zhu,[a] Zhengquan Li,[b] Hangxun Xu,*[a] and Yujie Xiong*[a]

Abstract: Quantum dots (QDs), a class of promising candidates for harvesting visible light, generally exhibit low activity and selectivity toward photocatalytic CO_2 reduction. Anchoring QDs with metal complexes (or metal cations through ligands) is a widely used strategy for improving their catalytic activity; however, it suffers from low selectivity and stability in CO_2 reduction. Herein, we report that doping CdS QDs with transition metal sites can overcome these limitations to achieve highly selective photocatalytic reactions of CO_2 with H_2O (100% to CO and CH_4), with excellent durability over 60 h. Doping Ni sites into CdS lattice can effectively trap photoexcited electrons at surface catalytic sites and substantially suppress H_2 evolution. The method reported here can be extended to various transition metal sites, and offers new opportunities for exploring QDs-based earth-abundant photocatalysts.

Sunlight-driven CO_2 conversion is an appealing approach to mitigate the impact of greenhouse gases on the environment.[1-3] As compared with the conventional light harvesters of inorganic oxides, metal chalcogenide quantum dots (QDs) possess many attractive features such as high extinction coefficients, multiple-exciton generation effects, tunable bandgaps and rich surface-binding sites,[4-6] emerging as a class of excellent candidates for visible-light photocatalysis.[7,8] Due to the lack of intrinsic catalytic sites, these QDs-based photocatalysts have to anchor metal complexes to achieve CO_2 reduction. However, the organic ligands are unfavorable for shuffling photo-generated charges for surface reactions.[6,9] Moreover, the dangling bonds derived from the detachment of metal complexes from QDs form surface defect states at the QDs, which consequently reduces reaction activity and selectivity at catalytic sites.[7] Thus directly implanting catalytic sites into light-harvesting centers (i.e., QDs) could be an ideal solution to shorten electron transfer pathway as well as enhance the durability of photocatalysts by excluding the use of bridging ligands.

Doping is a very versatile route to implant metal cations into QDs. The dopants can create electronic states in the midgap region of QDs, which may in turn promote charge migration to surface and locally trap photoexcited electrons on surface.[10,11] As such, bulk recombination – a process detrimental to photocatalysis can be markedly suppressed. Although various doped QDs have been utilized for photocatalytic H_2 production and organic pollutant degradation,[12-15] it remains largely unexplored for CO_2 photoreduction. The reduction of protons in water to H_2 mainly competes with the CO_2 reduction in such a system. Thus it would be fundamentally important to explore whether the activity and selectivity for CO_2 reduction can be improved by doping QDs with transition metal cations.

Herein, we report a highly selective and durable system for CO_2 photoreduction with Ni^{2+}-doped CdS QDs (namely, Ni:CdS QDs). Our investigation based on various characterization techniques reveals that the incorporation of Ni sites into CdS lattice can effectively trap photoexcited electrons at surface catalytic sites and substantially suppress H_2 evolution. As a result, the selectivity of CO_2 reduction *versus* H_2 evolution reaches 100%, and the catalyst exhibits excellent durability for more than 60 h.

Ni:CdS QDs are obtained by simply introducing Ni^{2+} cations into the synthesis of CdS QDs (see details in SI). Transmission electron microscopy (TEM) (Figure S1) reveals that the particle size of CdS QDs is maintained around 6.6 nm after Ni doping. Such a low concentration of Ni dopants does not alter the cubic structure and crystallinity of CdS QDs (Figure S2). As determined by UV-vis diffuse reflectance spectroscopy (Figure S3), the bandgap of pristine CdS QDs is ~2.43 eV (Figure 1a), which has not been much altered after Ni doping. We further estimate the positions of conduction band edge (E_{CB}) through a linear sweep voltammetry (LSV) technique according to the peaks for lattice Cd^{2+} reduction potentials (Figure 1b).[16,17] Pristine CdS QDs only exhibit one peak assigned to reduction potential of Cd^{2+}/Cd^0 at -0.95 V *versus* NHE, while two reduction peaks appear at -1.03 and -0.63 V for Ni:CdS QDs. As a result, the E_{CB} for CdS and Ni:CdS QDs should be located around -0.95 V and -1.03 V, respectively, in good agreement with previous assignments.[16,17] As such, the valence band edge (E_{VB}) can be determined as illustrated in Figure 1c. Notably, the additional reduction peak at -0.63 V *versus* NHE can be assigned to reduction potential of Ni^{2+}/Ni^0 on the surface of QDs.[18] This designates that photoexcited electrons can be transferred to surface Ni sites for CO_2 reduction.

In addition to the doping approach, we prepare two reference samples (Figure 1d): the CdS QDs anchored with Ni^{2+} through bridging ligands (namely, CdS-b-Ni),[8] and the CdS

---

[a] Dr. J. Wang,[+] T. Xia,[+] L. Wang, Dr. X. Zheng, Dr. Z. Qi, Dr. C. Gao, Prof. J. Zhu, Prof. H. Xu, Prof. Y. Xiong
Hefei National Laboratory for Physical Sciences at the Microscale, *i*ChEM (Collaborative Innovation Center of Chemistry for Energy Materials), School of Chemistry and Materials Science, and National Synchrotron Radiation Laboratory
University of Science and Technology of China
Hefei, Anhui 230026, P. R. China
E-mail: yjxiong@ustc.edu.cn; hxu@ustc.edu.cn
[b] Dr. J. Wang,[+] Prof. Z. Li
Key Laboratory of the Ministry of Education for Advanced Catalysis Materials, Zhejiang Normal University
Jinhua, Zhejiang 321004, P. R. China

[+] These authors contributed equally to this work.

Supporting information for this article is given via a link at the end of the document.

QDs mixed with Ni^{2+} in solution that reaches QD surface through random collision (namely, CdS-Ni).[19] The ligands in CdS-b-Ni bridge Ni^{2+} cations with CdS QDs so that the photoexcited electrons in QDs can be transferred to the anchored metal cations (Figure S4-S6).[20,21] In the case of CdS-Ni, a small amount of Ni^{2+} can be adsorbed on the surface of CdS QDs and serve as catalytic sites.[22] Figure 2a shows that the selectivity for CO_2 reduction to CO/CH_4 *versus* H_2O reduction to H_2 impressively approaches 100% by Ni:CdS QDs among various samples. The CO_2 reduction rate by Ni:CdS QDs is about 4.9 and 3.9 times higher than those by CdS-Ni and CdS-b-Ni systems, respectively. This indicates that doping Ni into CdS QDs can dramatically suppress H_2 evolution. Note that a trace amount of CO and H_2 is generated by pristine CdS QDs, so the doped Ni^{2+} cations may serve as catalytic sites for CO_2 reduction.

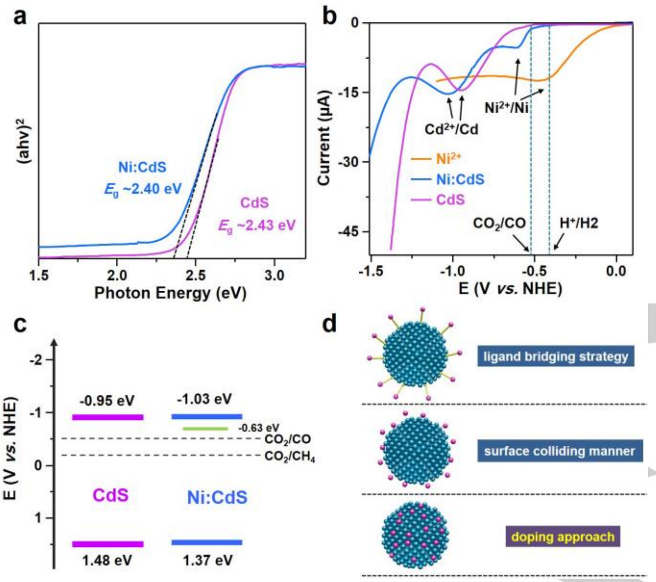

Figure 1. a) The bandgaps of CdS QDs and Ni:CdS QDs. b) LSV curves of CdS QDs, Ni:CdS QDs and free Ni^{2+} cations in water under identical conditions. c) Energy band diagrams for CdS QDs and Ni:CdS QDs with respect to the CO_2 reduction potentials (pH ~7). d) Schematic illustration for three different configurations of combining QDs with metal cations.

We further look into the effect of dopant concentration on photocatalytic performance as the properties of QDs are often tuned by dopant concentrations.[13] Figure 2b shows the photocatalytic performance of Ni:CdS QDs at the Ni contents from 0.12% to 1.03%, in which a volcano tendency is observed for the photocatalytic activity with the maximum at 0.26% by continuously increasing the amount of Ni dopants. Notably Ni(0.26%):CdS QDs achieve a turnover number (TON) of ~35 and ~300 in terms of Ni atoms and QDs, respectively, which turns out to be stable in five 12-hour cycles (i.e., 60 h in total, Figure 2c). In comparison, the catalytic activity for CdS-b-Ni begins to significantly decay in the second cycle (Figure S7). The strong metal-sulfur binding in lattice can avoid the leaching of Ni^{2+} cations from Ni:CdS QDs,[23] which appears as an advantage over metal complex catalysts (Figure S7). The isotopic-label experiment using $^{13}CO_2$ as substrate (Figure 2d) confirms that the carbon source of CO and CH_4 indeed originates from photocatalytic CO_2 reduction by Ni:CdS QDs, while no CO or CH_4 can be detected under Ar atmosphere.

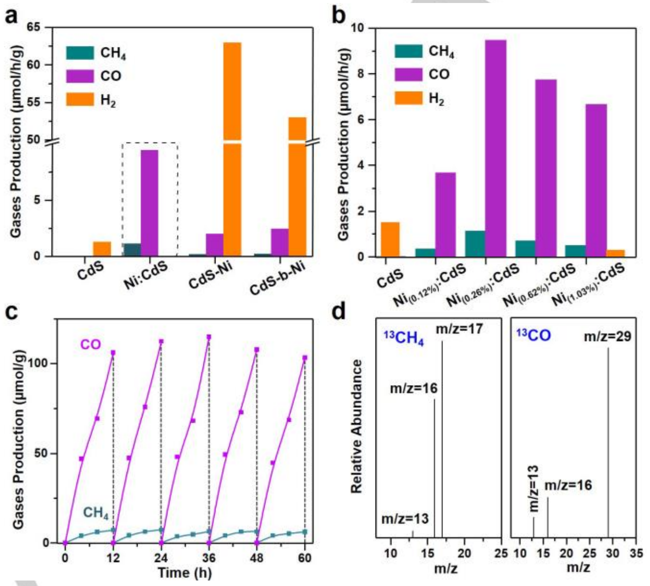

Figure 2. a) Average production rates of CH_4, CO and H_2 using various photocatalysts based on CdS QDs. b) Average production rates of CH_4, CO and H_2 by CdS QDs at various Ni doping amounts. c) Cycling production of CH_4 and CO using Ni(0.26%):CdS QDs. d) Mass spectra of $^{13}CH_4$ (m/z = 17) and ^{13}CO (m/z = 29) produced over Ni(0.26%):CdS QDs in the photocatalytic reduction of $^{13}CO_2$.

To elucidate the roles of Ni dopants in enhancing photocatalytic CO_2 reduction, we first examine the charge behaviors in QDs that are often regulated through metal doping. Both pristine CdS QDs and Ni:CdS QDs exhibit a photoluminescence (PL) around 600 nm (Figure 3a). Such a PL should originate from the radiative electron-hole recombination on their surface rather than in bulk. This argument is supported by the PL spectra collected in the presence of methyl viologen (MV^{2+}) – an agent to sacrifice surface electrons of QDs, which displays a weak emission peak for the radiative recombination in bulk at 500-550 nm (Figure 3b). Typically, enhanced surface photoemission indicates that more photoexcited electrons can reach QD surface for radiative recombination with the holes in valence band, rather than being trapped inside the QDs.[10,11,14] Here, Ni doping can enhance the PL around 600 nm (Figure S8), as more photoexcited electrons are transferred to surface and trapped at surface metal sites for surface-states emission.[10,11,14] In a practical photocatalytic CO_2 reduction, the photoexcited electrons trapped at surface Ni sites would participate in the reactions with Ni atoms as catalytic centers. However, the PL intensity of Ni:CdS QDs around 600 nm is reduced when further increasing the doping concentration of Ni, as photoexcited electrons are more trapped at bulk Ni sites and participate in non-radiative recombination (also see PL decay in Figure S9 and Table S1). It is worth pointing out that the formation of NiS is another cause for the deteriorative photocatalytic performance at a very high doping concentration (Figure S10-S13).

10.1002/anie.201810550

The PL measurements have highlighted the process for transferring photoexcited electrons from CdS to Ni sites. Electron spin resonance (ESR) spectroscopy is further employed to examine the local electronic state of Ni^{2+} (Figure 3c). Ni(0.26%):CdS QDs give a typical ESR signal in dark that can be ascribed to the high-spin state of Ni^{2+} (g = 2.1).[24] After irradiated for 2 min, the signal for Ni^{2+} in Ni:CdS QDs is substantially reduced, which can be assigned to the lowered spin state by the reduction of Ni^{2+}. In contrast, no distinct ESR signal can be detected for pristine CdS QDs. This observation confirms that photogenerated electrons are transferred from QDs to Ni^{2+} centers upon photoexcitation. Moreover, near-edge X-ray absorption fine structure (NEXAFS) spectroscopy (Figure 3d) reveals that the binding energies for Ni:CdS QDs are 0.5 eV higher than those for pristine CdS QDs, indicating a decrease in electron density for sulfur.[25] This demonstrates that the photoexcited electrons trapped by Ni^{2+} are mainly supplied by sulfur. Accordingly, varying Cd/S stoichiometry is able to control the number of sulfur vacancies that trap photoexcited electrons (Figure S14-S16 and Table S2-S4).[26] In photocatalytic CO_2 reduction, the surface Ni sites in sulfur vacancies would receive the photoexcited electrons to trigger the reduction of adsorbed CO_2 molecules so that a higher Cd/S ratio can benefit photocatalytic CO_2 reduction.

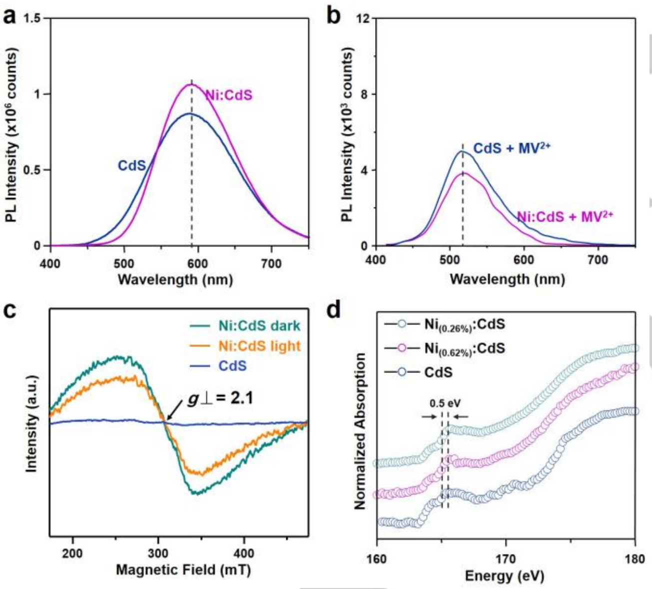

Figure 3. a) PL emission spectra of bare CdS and Ni(0.26%):CdS QDs (λ_{ex}= 380 nm). b) PL emission spectra of bare CdS and Ni(0.26%):CdS QDs in the presence of MV^{2+} (10^{-5} M, λ_{ex}= 380 nm). c) ESR spectra of bare CdS and Ni(0.26%):CdS QDs. d) S $L_{2,3}$-edge NEXAFS spectra of bare CdS and Ni:CdS QDs.

Based on the information above, we can depict the process of electron transfer as Figure S17. When the electrons in CdS QDs are photoexcited, they will be transferred to surface and relax to surface defect states. This electron trapping by surface sulfur vacancies becomes prominent at a high ratio of Cd/S (Figure S15). In comparison, the photoexcited electrons in Ni:CdS QDs will be transferred to the doped Ni atoms in sulfur vacancies and relax to shallow charge trap states. At a low dopant concentration (Figure S8), the electrons are mainly trapped at the surface Ni sites in the vacancies. The addition of Ni dopants can enhance the electron trapping in sulfur vacancies (Figure 3a) so as to substantially promote charge separation, as confirmed by photocurrent and transient open-circuit voltage decay measurements (Figure S18 and S19).

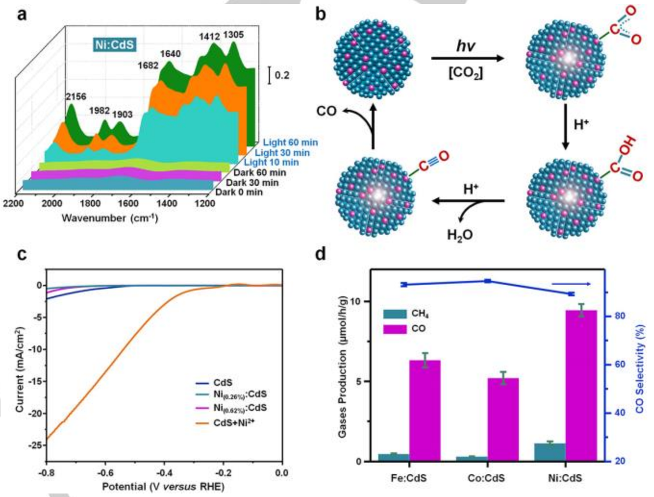

Figure 4. a) *In-situ* DRIFTS spectra for the reactions of CO_2 with H_2O on Ni(0.26%):CdS QDs under irradiation. b) Schematic illustration for the proposed mechanism of photocatalytic CO_2 reduction at Ni:CdS QDs. c) Electrochemical polarization curves for HER using various samples in PBS buffer solution (pH = 7). d) Average production rates of CH_4, CO and H_2 by CdS QDs doped with different metal cations.

The improvement of charge separation and transfer by doping is critical to promote photocatalytic activity; however, it remains unclear why the selectivity for CO_2 reduction can be improved. The evolution of CO_2 and H_2O gas at catalytic sites is investigated by employing *in-situ* diffuse reflectance infrared Fourier-transform spectroscopy (DRIFTS) (Figure 4a and S20). Along with light irradiation, the peaks located from 1200 to 2200 cm^{-1} arise with the gradually increased intensity for CdS-Ni, CdS-b-Ni and Ni:CdS QDs due to the formation of intermediate carbonate species (Table S5).[27,28] Thus the mechanism for Ni:CdS QDs in photocatalytic CO_2 can be outlined in Figure 4b. In the first step, Ni^{2+} adsorbs a CO_2 molecule and captures two electrons to give a Ni-CO_2 complex as resolved by the feature at 1682 cm^{-1}.[7] The second step is to form Ni-COOH by accepting a proton from the surrounding medium, corresponding to the peaks located at 1305 cm^{-1}, 1412 cm^{-1} and 1640 cm^{-1} for C–OH, C–O and C═O stretching, respectively.[29] Subsequently, the Ni-COOH accepts another proton and undergoes dehydration to form a Ni-CO complex which exhibits two additional stretching peaks at 1903 and 1982 cm^{-1}.[7] The CO molecule in Ni-CO can be readily released and desorbed from the surface of QDs as indicated by the peak appearing at 2156 cm^{-1}.[30] Intuitively, the minor product of CH_4 should originate from the hydrogenation at the Ni-CO complex. During this process, the QDs with a high Cd/S ratio offer abundant coordinatively unsaturated Ni sites for

CO_2 adsorption and activation on surface, which boosts the overall photocatalytic performance (Figure S14). Notably, the peak intensity variation for Ni:CdS QDs is substantially higher than the other three catalysts, manifesting the higher activity of Ni:CdS in photocatalytic CO_2 reduction.

Electrocatalytic measurements (Figure 4c) show that hydrogen evolution reaction (HER) on Ni:CdS is dramatically lower than that by CdS QDs mixed with free Ni cations – a similar situation to CdS-Ni in photocatalytic measurements. This indicates that the doping of Ni sites into CdS lattice is a way to suppress HER, most likely because the doped Ni sites can be more affected by the electronic structure of CdS QDs. The unique role of Ni species as catalytic centers is further proven by control experiments using CdS shielding and in the presence of free Ni^{2+} cations (Figure S21 and S22). It is evident that this doping strategy is a prominent method for fixing metal cations uniformly on surface of QDs and can be extended to other divalent transition metals such as Fe^{2+} and Co^{2+} (Figure 4d).

In summary, we have successfully demonstrated that doping QDs, the most common strategy applied to tune the photophysical properties of QDs, can markedly reduce CO_2 into CO and CH_4 with a nearly 100% selectivity, a TON of ~35 in terms of Ni atoms and an excellent durability for more than 60 h. The doped metal sites play a dual role in the photocatalytic process – trapping photoexcited electrons at surface catalytic sites and suppressing H_2 evolution. This work is the first experimental report that doping QDs with metal cations can lead to efficient photocatalytic systems for reducing CO_2 with high selectivity and durability, which provides insights into simultaneously maneuvering the two key steps – charge transfer and separation, and surface reactions through a single component. It offers us a valid approach to earth-abundant photocatalysts for CO_2 photoreduction using visible light.

Experimental Section

See Supporting Information for material synthesis and characterization methods.

Acknowledgements

This work was financially supported in part by National Key R&D Program of China (2017YFA0207301), NSFC (21725102, 21471141, U1532135, 21701143, 21875235), CAS Key Research Program of Frontier Sciences (QYZDB-SSW-SLH018), and CAS Interdisciplinary Innovation Team.

Keywords: photocatalysis • quantum dots • catalytic sites • doping • CO_2 reduction

[1] J. L. White, M. F. Baruch, J. E. Pander, Y. Hu, I. C. Fortmeyer, J. E. Park, T. Zhang, K. Liao, J. Gu, Y. Yan, T. W. Shaw, E. Abelev, A. B. Bocarsly, *Chem. Rev.* **2015**, *115*, 12888–12935.
[2] T. Inoue, A. Fujishima, S. Konishi, K. Honda, *Nature* **1979**, *277*, 637–638.
[3] K. K. Sakimoto, A. B. Wong, P. Yang, *Science* **2016**, *351*, 74–77.
[4] A. P. Alivisatos, *Science* **1996**, *271*, 933–937.
[5] D. V. Talapin, J. S. Lee, M. V. Kovalenko, E. V. Shevchenko, *Chem. Rev.* **2010**, *11*, 389–458.
[6] R. D. Harris, S. B. Homan, M. Kodaimati, C. He, A. B. Nepomnyashchii, N. K. Swenson, S. C. Lian, R. Calzada, E. A. Weiss, *Chem. Rev.* **2016**, *116*, 12865–12919.
[7] M. F. Kuehnel, K. L. Orchard, K. E. Dalle, E. Reisner, *J. Am. Chem. Soc.* **2017**, *139*, 7217–7223.
[8] S. C. Lian, M. S. Kodaimati, D. S. Dolzhnikov, R. Calzada, E. A. Weiss, *J. Am. Chem. Soc.* **2017**, *139*, 8931–8938.
[9] D. A. Hines, P. V. Kamat, *J. Phys. Chem. C* **2013**, *117*, 14418–14426.
[10] P. K. Santra, P. V. Kamat, *J. Am. Chem. Soc.* **2012**, *134*, 2508–2511.
[11] D. J. Norris, A. L. Efros, S. C. Erwin, *Science* **2008**, *319*, 1776–1779.
[12] Y. Dong, J. Choi, H. K. Jeong, D. H. Son, *J. Am. Chem. Soc.* **2015**, *137*, 5549−5554.
[13] M. Luo, Y. Liu, J. Hu, H. Liu, J. Li, *ACS Appl. Mater. Interf.* **2012**, *4*, 1813–1821.
[14] H. M. Huang, B. Y. Dai, W. Wang, C. H. Lu, J. H. Kou, Y. R. Ni, L. Z. Wang, Z. Z. Xu, *Nano Lett.* **2017**, *17*, 3803–3808.
[15] R. Shi, H. F. Ye, F. Liang, Z. Wang, K. Li, Y. X. Weng, Z. S. Lin, W. F. Fu, C. M. Che, Y. Chen, *Adv. Mater.* **2018**, *30*, 1705941.
[16] T. Simon, N. Bouchonville, M. J. Berr, A. Vaneski, A. Adrovic, D. Volbers, R. Wyrwich, M. Doblinger, A. S. Susha, A. L. Rogach, F. Jackel, J. K. Stolarczyk, J. Feldmann, *Nat. Mater.* **2014**, *13*, 1013–1018.
[17] J. Zhao, M. A. Holmes, F. E. Osterloh, *ACS Nano* **2013**, *7*, 4316–4325.
[18] Z. J. Han, F. Qiu, R. Eisenberg, P. L. Holland, T. D. Krauss, *Science* **2012**, *338*, 1321–1324.
[19] *X. Meng, Q. Yu, G. Liu, L. Shi, G. Zhao, H. Liu, P. Li, K. Chang, T. Kako, J. Ye, Nano Energy* **2017**, *34*, 524–532.
[20] S. P. Wang, N. Mamedova, N. A. Kotov, W. Chen, J. Studer, *Nano Lett.* **2002**, *2*, 817–822.
[21] B. M. Graff, B. P. Bloom, E. Wierzbinski, D. H. Waldeck, *J. Am. Chem. Soc.* **2016**, *138*, 13260–13270.
[22] G. Zhao, Y. Sun, W. Zhou, X. Wang, K. Chang, G. Liu, H. Liu, T. Kako, J. Ye, *Adv. Mater.* **2017**, *29*, 1703258.
[23] A. Nag, D. S. Chung, D. S. Dolzhnikov, N. M. Dimitrijevic, S. Chattopadhyay, T. Shibata, D. V. Talapin, *J. Am. Chem. Soc.* **2012**, *134*, 13604–13615.
[24] G. Liu, P. Li, G. Zhao, X. Wang, J. Kong, H. Liu, H. Zhang, K. Chang, X. Meng, T. Kako, J. Ye, *J. Am. Chem. Soc.* **2016**, *138*, 9128–9136.
[25] M. Han, Y. Luo, J. E. Moryl, R. M. Osgood Jr., J. G. Chen, *Surf. Sci.* **1998**, *415*, 251–263.
[26] P. V. Kamat, N. M. Dimitrijević, R. W. Fesseden, *J. Phys. Chem.* **1987**, *91*, 396–401.
[27] E. M. Köck, M. Kogler, T. Bielz, B. Klötzer, S. Penner, *J. Phys. Chem. C* **2013**, *117*, 17666–17673.
[28] C. Amatore, J.-M. Savéant, *J. Am. Chem. Soc.* **1981**, *103*, 5021–5023.
[29] N. J. Firet, W. A. Smith, *ACS Catal*. **2017**, *7*, 606–612.
[30] W. G. Su, J. Zhang, Z. Feng, T. Chen, P. Ying, C. Li, *J. Phys. Chem. C* **2008**, *112*, 7710–7716.

Entry for the Table of Contents

COMMUNICATION

Quantum dots (QDs), a class of promising candidates for harvesting visible light, commonly possess low activity and selectivity toward photocatalytic CO_2 reduction. Doping CdS QDs with transition metal cations, which can trap photoexcited electrons and suppress H_2 evolution, provides an approach to visible-light-driven highly selective CO_2 reduction with excellent durability.

Jin Wang, Tong Xia, Lei Wang, Xusheng Zheng, Zeming Qi, Chao Gao, Junfa Zhu, Zhengquan Li, Hangxun Xu, and Yujie Xiong**

Page No. – Page No.

Enabling Visible-Light-Driven Selective CO_2 Reduction by Doping Quantum Dots: Trapping Electrons and Suppressing H_2 Evolution